34th Annual International Conference of the IEEE EMBS
San Diego, California USA, 28 August - 1 September, 2012

# Automated System for Imageless Evaluation of Arterial Compliance

Ashish Kumar Sahani, Jayaraj Joseph and Mohanasankar Sivaprakasam

*Abstract*—**Evaluation of arterial compliance is very significant in early detection of coronary heart disease. Here we present an imageless portable system for automated estimation of local arterial compliance, designed to be operated by a general medical practitioner with no prior knowledge of ultrasonography. An algorithm for automatic detection and tracking of the arterial wall locations has been developed to minimize the operator expertise required for measurement. The performance of the automated algorithm was thoroughly characterized using a simulation platform developed for the purpose. Measurements performed on a few human volunteers by untrained personnel clearly illustrated the practical utility of the automatic algorithm during in-vivo tests. The proposed system could be used for developing an inexpensive cardiovascular screening device for large scale deployment in primary health care centers.**

***Keywords-arterial wall detection; arterial distension; local arterial compliance; ultrasound measurement; carotid artery***

## I. Introduction

Non-invasive evaluation of the arterial compliance for the common carotid artery (CCA) has been established to be very significant in early detection of coronary heart disease (CHD) [1]. Given the high incidence of CHD in the developing nations, a low cost screening device based on arterial compliance measurement, that can be used by a general practitioner is very desirable [2]. The use of B-mode ultrasound images for this measurement puts a premium on both the hardware required for data processing and also on the operator expertise necessary for identification of the arterial wall [3]. We had earlier demonstrated the feasibility of a single element ultrasound transducer in the measurement of arterial distension [4].

Here we present an imageless system for automated evaluation of arterial compliance with a new algorithm for automatic detection and tracking of the arterial wall locations. A parametric analysis is performed using a dedicated simulation platform to thoroughly evaluate the performance of the wall detection and wall-tracking algorithms. The in-vivo performance of the proposed system is also evaluated to verify the practical utility of the system operated by untrained personnel. The arterial compliance measures of a few human volunteers measured during in-vivo tests are also presented.

## II. Hardware Description

The hardware architecture of the system built for use with a single element ultrasound transducer has already been presented in our previous work [4]. A set of 5 V digital pulses generated with an Atmega-8 (Atmel) microcontroller is utilized by the transducer driver to generate sharp high voltage pulses which excite the ultrasound transducer (V110 RM, Panametrics NDT) at its resonant frequency of 5 MHz ($f_{us}$) [4]. The echo signal is received by the same transducer and is filtered (1st order high pass filter with cutoff 100 KHz), amplified (pre-amp with gain 40 dB) and digitized at 100 MS/s using a NI-USB-5133 scope (National Instruments). The pulse repetition time ($t_{pr}$) is 10 ms. Brachial artery systolic and diastolic pressures ($P_{bs}$ and $P_{bd}$), measured by using an automatic blood pressure monitor (HEM-7101, OMRON), is used to estimate the carotid pressure for calculation of arterial compliance estimates.

## III. Data Acquisition and Signal Characteristics

The transducer is placed over the patient's neck approximately 2 cm below the carotid bulb. After every $t_{pr}$ seconds a pulse is fired and N data points are acquired for next $t_{aq}$ seconds ($N = t_{aq} \times f_s$). After $M \times t_{pr}$ seconds we have M rows of N points each. The signal processing algorithm uses this M x N matrix $R$ containing raw data as input (Fig. 1). The system searches for pair of pulsating walls, to provide real-time assistance to the operator, in placement of the probe through binary indicators. Echoes observed in the received signal (Fig. 2) arise from specular reflection at the following types of scattering structures.

i. Fixed structures and skin-gel interface which show up as static echoes ($S_E$).
ii. Adjacent echoes moving in opposite directions, that correspond to the proximal and distal walls of the artery ($M_W$).

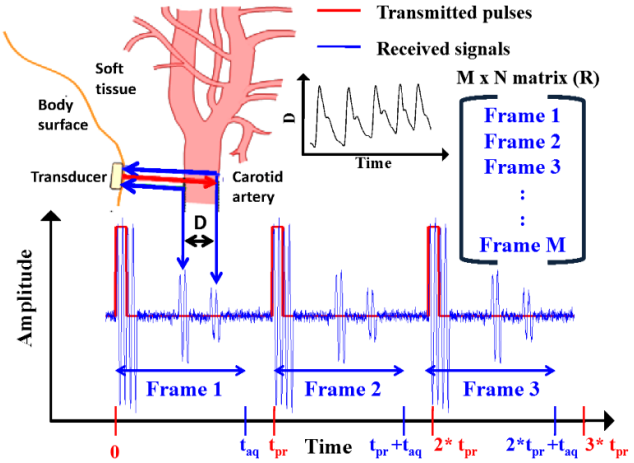


Figure 1. Illustration of the transducer placement and signal characterisation. The structure of matrix $R$ and distension of artery is also shown.

*All authors are with Department of Electrical Engineering, Indian Institute of Technology, Madras, Chennai, India (phone: +91 9445826433; e-mail: ashishkumarsahani@gmail.com).

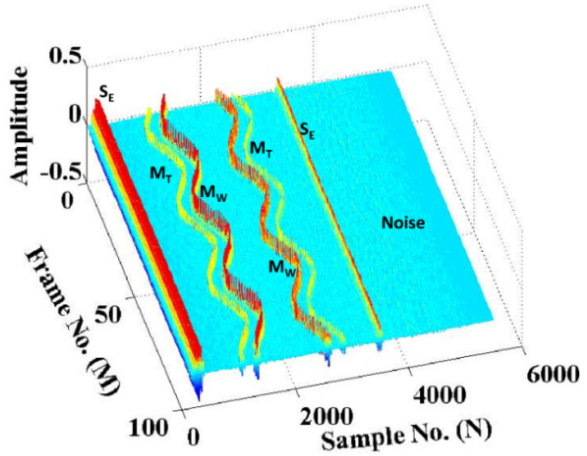


Figure 2. A simulated frame (SNR = 10 dB) with the movement of the arterial wall echoes visualized over successive acquisitions.

iii. Echogenic tissues near the artery that are pushed into motion by its pulsating walls ($M_T$).
iv. Noise.

The algorithm uses this motion cue (ii) for validating the correct positioning of the probe and identifying the approximate wall positions for tracking.

## IV. Signal Processing Algorithm

Apart from the regular wall motion tracking, the signal processing algorithm in an imageless compliance system has to perform the additional task of assisting the user to place the probe over the CCA correctly and automatically identify the approximate arterial wall locations. The overall measurement algorithm has two important stages, viz. (i) Wall detection stage, in which the artery is identified and approximate wall locations are determined, and (ii) Motion tracking stage, in which the movement of arterial walls are tracked to obtain the distension waveform.

The overall block diagram of the two stages is illustrated in Fig 3. As the operator slides the probe over different expected locations on patient's neck, M rows of data are acquired and passed into the wall detection algorithm as matrix *R*. Each row of *R* is filtered with a 5th order band pass filter. Then a non-linear gain is applied to suppress high amplitude reflections from skin gel interface. The algorithm tries to identify the wall positions (*Wall1* and *Wall2*) and if successful, asserts an LED indicator. This means that the artery has been found and the operator must hold the probe steadily at the same position until enough data is acquired for reliable compliance measurement. If no artery is found then algorithm goes on to reload *R* by acquiring next M rows of data and repeats the procedure. The value of M is kept small (typically 2 to 10) to enable fast processing of *R* thereby facilitating the real time placement of probe and automatic identification of approximate wall locations. If artery is found, then the algorithm moves into the second stage. Two windows are placed around *Wall1* and *Wall2*. The features in the windows are tracked over successive M′ frames using correlation window based technique [4]. Two waveforms corresponding to the positions of the two walls are obtained. As artery walls move in opposite directions, the two waveforms are negatively correlated.

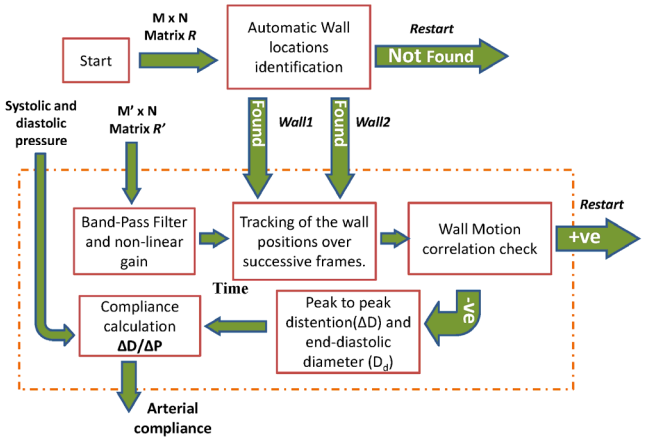


Figure 3. Motion tracking stage of the signal processing algorithm.

It is possible that user may lose the artery location due to hand motion or patient's movement. This check ensures additional fidelity of measurement. Finally, arterial distension and arterial compliance are measured by standard methods.

### A. *Automatic identification of approximate arterial wall locations*

The *R* matrix (after filtering and application of non-linear gain) is the input to this algorithm. It is a MxN matrix whose row and column indices are $m \in [0, \mathrm{M}-1]$ *and* $n \in [0, \mathrm{N}-1]$ respectively. Let $m^{th}$ row of *R* be denoted by $F_m$. We calculate a sliding window covariance $\mathrm{SWC_m}$ with a window length of W of each $F_m$ and $F_{m-1}$ frame as defined in (1).

$$\mathrm{SWC_m(n)} = \frac{\sum_{k=n-\left\lfloor \frac{\mathrm{W}}{2} \right\rfloor}^{k=n+\left\lfloor \frac{\mathrm{W}}{2} \right\rfloor} F_{(m-1)}(k) \times F_m(k)}{\mathrm{W}} \qquad (1)$$

$$for,\ \left\lfloor \frac{\mathrm{W}}{2} \right\rfloor < n < \mathrm{N} - \left\lfloor \frac{\mathrm{W}}{2} \right\rfloor,\ \mathrm{W}\ is\ odd$$

$$= 0, \qquad for, \qquad all\ other\ n < N$$

The $\mathrm{SWC_m}$ curve is then normalized between 0 and 1 (Fig. 4). $\mathrm{SWC_m(n)} \approx 0$ for all $m$, at any $n$ corresponding to noise locations because covariance of noise is very small. It shows distinct peaks at any *n* corresponding to significant structures. The typical ratio between value of peaks of $\mathrm{SWC_m}$ at *n* corresponding to echo and noise is typically 100:1. The very small values of $\mathrm{SWC_m}(n)$, at any *n* corresponding to noise is eliminated by using a fixed threshold. We smooth each $\mathrm{SWC_m}$ and detect the peaks by using a second derivative based peak detection algorithm. Assuming the two walls are always more than more than 4 mm apart [5], we eliminate the smaller peak out of any two peaks placed less than 2 mm apart. Let L peak locations detected for $\mathrm{SWC}_m$ be denoted as $P_{m0}, P_{m1}, \ldots P_{ml}, \ldots, P_{m(\mathrm{L}-1)}$. There are significant echoes at each $P_{ml}$ in $F_{m-1}$ and $F_m$. For isolating moving echoes from static echoes using correlation based shift estimation between all L significant features in $F_0$ and $F_m$ (Fig. 5), we place windows $W_{0l}$ and $W_{ml}$ of length (2W+1), centered at each $\mathrm{P_{ml}}$ on $F_0$ and $F_m$ respectively, as defined in (2) and (3).

$$W_{0l}(k) = F_0(P_{ml} - \mathrm{W} + k), for\ k \in [0, 2\mathrm{W}] \quad (2)$$

$$W_{ml}(k) = F_m(P_{ml} - \mathrm{W} + k), for\ k \in [0, 2\mathrm{W}] \quad (3)$$

For each $F_m$ we define $S_m$ having L points, which is a measure of shift in the features at $P_{ml}$ between $F_0$ and $F_m$ by (4) and (5).

$$C_{ml}(p) = \sum_{\mathrm{k}=0}^{\mathrm{k}=2\mathrm{W}} W_{0l}(\mathrm{k}) \times W_{ml}(\mathrm{k}+\mathrm{p}) \quad (4)$$
$$for, p \in [-2\mathrm{W}, 2\mathrm{W}]\ and\ m \in [1, M-1]$$

$$S_m(l) = \text{index of max}\,(C_{ml}) \quad (5)$$

We are not interested in any static echoes so we delete all $S_m(l) = 0$ and corresponding $P_{ml}$. As the echoes of the walls of the carotid are adjacent to each other and shift in opposite direction we expect a zero crossing in each $S_m$ between some $S_m(l)$ and $S_m(l+1)$. We copy the corresponding $P_{ml}$ and $P_{m(l+1)}$ into two new column matrices $W1$ and $W2$ respectively, each having $(\mathrm{M}-1)$ rows (6).

$$if,\ S_m(l) \times S_m(l+1) < 0$$
$$then, W1(m) = P_{ml} \text{ and } W2(m) = P_{m(l+1)} \quad (6)$$

If there are more than one $l$ for which (6) is satisfied then we calculate the distance $D'$ between $P_{ml}$ and $P_{m(l+1)}$ for each such $l$ (7).

$$D' = \left(P_{m(l+1)} - P_{ml}\right)(c/2f_s) \quad (7)$$

where, $\mathrm{c} =$ sound velocity in tissue.

The zero crossing between $l$ and $l$+1 is considered to be valid only if $D_{min} < D' < D_{max}$. The limits of carotid diameter used for this check are well established [5]. If no valid peaks are detected or, if the detected peaks are located very close to the skin surface (within 1 mm) then we set $W1(m) = -1$ and $W2(m) = -1$. The final value of approximate wall locations $Wall1$ and $Wall2$ are found by taking the median of all positive values in $W1$ and $W2$. If $W1$ and $W2$ have no positive values then that means artery walls could not be located.

### B. *Estimation of wall motion and distension*

After the wall detection, M′ new frames of data are acquired and stored as the rows $G_m$ of the matrix $R'$. The approximate locations of the arterial walls ($Wall1$ and $Wall2$) obtained as a result of the wall-detection algorithm, is used to initialize a correlation based wall motion tracking algorithm [4]. The proximal and distal wall echoes are identified as in (8).

$$\text{Near Wall}_\mathrm{m}(\mathrm{k}) = \mathrm{G_m}(Wall1 - \mathrm{W} + \mathrm{k}) \quad (8a)$$
$$\text{Far Wall}_\mathrm{m}(\mathrm{k}) = \mathrm{G_m}(Wall2 - \mathrm{W} + \mathrm{k}) \quad (8b)$$
$$for\ k \in [0, 2\mathrm{W}]$$

The movement of the wall echoes in between successive acquisitions is estimated based on a shift and search algorithm utilizing a correlation based technique [4]. The estimated shifts between successive acquisitions are cumulatively added to estimate the proximal and distal wall motion waveforms $d_{nw}(m)$ and $d_{fw}(m)$. The arterial distension waveform $\Delta d(m)$ is then calculated as in (9).

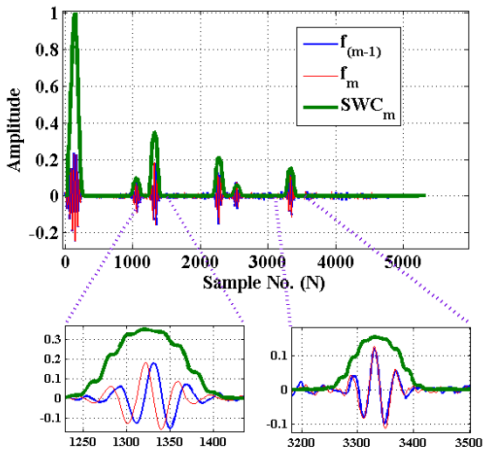


Figure 4. Representation of characteristics of $SWC_m$ curve overlayed over $f_m$ and $f_{m-1}$. It shows distinct peaks at all static and moving structures but very low amplitude at regions corresponding to noise.

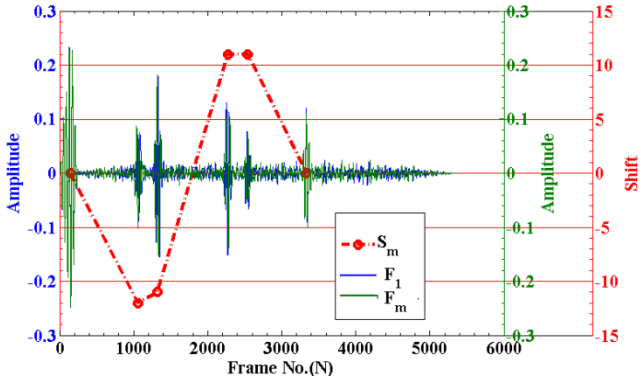


Figure 5. The value of $S_m(l)$ is illustrated here at differet peak locations ($P_m(l)$) for a particular $F_m$. This represents the shift of each significant echo from its position in $F_0$. Zero crossing in $S_m$ can be clearly observed.

$$\Delta d(m) = d_{fw}(m) - d_{nw}(m) \quad (9)$$
$$for, m \in [0, M'-1]$$

From the distension waveform the frame numbers corresponding to the minimum diameter are identified and the diastolic diameter ($D_d$) and systolic diameter ($D_s$) is estimated by method proposed in [4].

### C. *Wall motion negative correlation check*

We find the value of correlation $Q$ between $d_{nw}$ and $d_{fw}$ (10). As the two walls of the artery show opposing motion, this must be negative for the measurement to be valid.

$$Q = \frac{\langle d_{nw}\, d_{fw}\rangle - \langle d_{nw}\rangle\langle d_{fw}\rangle}{\sqrt{\left(\langle d_{nw}^2\rangle - \langle d_{nw}\rangle^2\right)\left(\langle d_{fw}^2\rangle - \langle d_{fw}\rangle^2\right)}} \quad (10)$$

where, $\langle X\rangle$ implies the mean of all elements of $X$

### D. *Compliance measurement*

Assuming the mean and diastolic pressure in the brachial ($P_{bm}$ and $P_{bd}$) and carotid arteries ($P_m$ and $P_d$) to be same and, considering the pressure change in the carotid artery to be proportional to its distension, we scale the systolic pressure value obtained from brachial artery

($P_{bs}$) to find the systolic pressure in carotid artery ($P_s$) [1], using (11).

$$P_s = \frac{P_{bs} \times (D_m - D_d)}{P_{bm} - P_{bs}} \quad (11)$$

Where, $D_m$ is the mean diameter of the artery

Using this value of systolic pressure $P_s$ compliance and distensibility is measured using (12), (13) and (14).

$$\Delta P = P_s - P_d \text{ and } \Delta D = D_s - D_d \quad (12)$$

$$\text{Compliance} = \Delta D/\Delta P \quad (13)$$

$$\text{Distensibility} = \Delta D/(\Delta P \times D_d) \quad (14)$$

## V. Performance Evaluation of the Algorithm

### A. Test-bench for Automatic wall detection

The functionality of the wall-detection algorithm is verified by using a test bench developed in Matlab®. The test bench generates data sets similar to the echo reflections obtained from CCA. The ultrasound pulses are modeled as Gaussian modulated sine waves and the echo signal is generated using weighted, time-shifted pulses [6]. From a pre-recorded noise sequence (measured from the experimental hardware), $N$ continuous samples are chosen starting from a random location, scaled in amplitude and added to the simulated signal to obtain various levels of signal to noise ratio (SNR). User can define rest locations ($W1_{Actual}$ and $W2_{Actual}$) of the artery walls, the shape of the motion waveform ($d_{nw}$ and $d_{fw}$) and maximum peak to peak amplitude $\Delta D$. Arterial wall motion is simulated by generating a two dimensional array of echo signals with motion profiles that can be sinusoidal, triangular or user defined. Parameters for static echoes and other moving echoes can also be specified. For the simulation studies, the following parameters were kept constant to match with the configuration of our experimental hardware setup, viz. $f_{us} = 5\ MHz, f_s = 100\ MHz,\ t_{pr} = 10\ ms$, and $N = 5333$.

### B. Benchmarking criteria

The ability of the wall-detection algorithm to correctly identify the approximate locations of the arterial walls is quantified in terms of Hit-rate (16). A Hit implies that the algorithm is able to find the locations of the arterial walls within reasonable limit of the wall's mean location ($W1_{Actual}$ and $W2_{Actual}$). A Hit is defined to have occurred if equation (15a) and (15b) are satisfied.

$$|W1_{Actual} - Wall1| < \Delta D \quad (15a)$$

and, $$|W2_{Actual} - Wall2| < \Delta D \quad (15b)$$

$$\text{Hit Rate} = \text{No. of Hits} \times 100/N_{meas} \quad (16)$$

Here $N_{meas}$ is the number of measurements performed for each combination of values of variables. All results are reported for $N_{meas}$ = 100. M new frames with different set of noise are generated for each individual measurement. Results of parametric analysis are reported in next section.

All measurements are done by varying the characteristics of signal shown in Fig. 1. Parameters are SNR, number of frames for each individual measurement (M), 3 dB pulse width of echo signal ($PW_{3dB}$), window length (W) and Frequency of oscillation of walls ($f_o$). All simulations are done with sinusoidal wall distension waveform having peak to peak amplitude ($\Delta D$) of 500 µm.

### C. Performance of the wall-detection algorithm

It can be seen from Fig. 6 that the algorithm is able to correctly identify the wall locations for SNR levels as low as 5 dB, with Hit-rate more than 90 %, for wall motion frequencies in the range of 0.6 – 4 Hz. The Hit-rate improves at larger SNR levels and at higher motion frequencies.

From Fig. 8 it is observed that at low SNR situations Hit-rate can be improved by considering more frames per measurement. We have to make a trade-off between Hit-rate and number of frames per trial (M), considering the speed requirement of in-vivo measurements. Offline measurements can always use more number of frames.

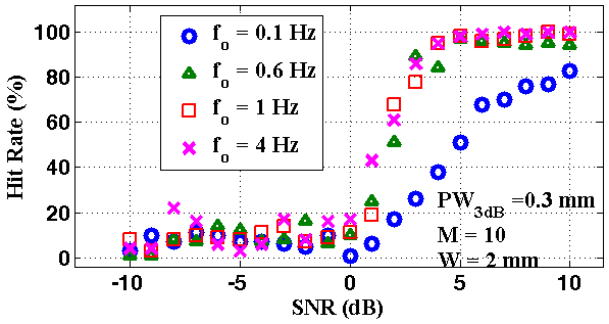


Figure 6. Hit-rate vs SNR at different frequency of motion of the artery.

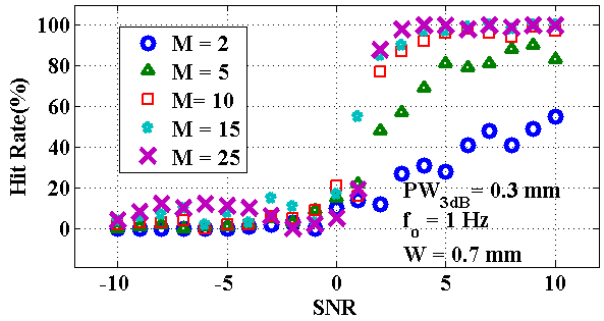


Figure 7. Hit-rate vs SNR at different No. of Frames per measurement.

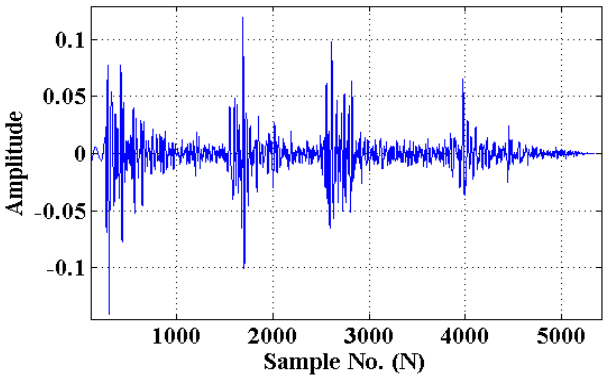


Figure 8. The ultrasound echo signal received after reflection from the carotid artery of volunteer A.

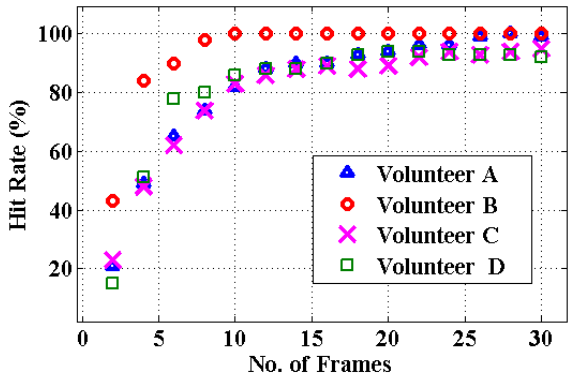


Figure 9. Wall-detection Hit-rate during in-vivo measurements by employing different No. of frames at W = 2mm.

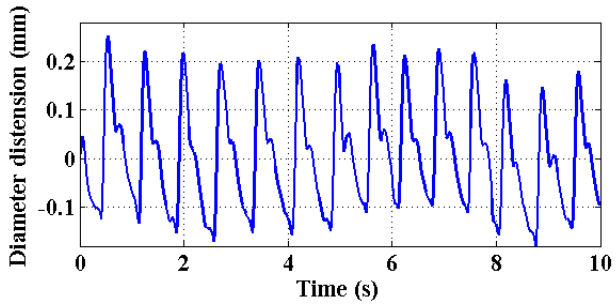


Figure 10. Distension waveform of volunteer A.

Hit-rate has a flat response over a wide range of window length (W) but performance drops at very small and very large window lengths. Window length in the range between two to four times the peak to peak distension of artery is preferred. Very small windows cannot cover the complete distension cycle, and for very large window lengths SWC will not have very distinct peaks for closely spaced echoes.

## VI. Results from Human Trials

### A. Validation of wall detection algorithm

The practical utility of the wall-identification algorithm was verified by measurements performed on a few volunteers. Artery wall locations ($W1_{User}$ and $W2_{User}$) were identified by the operator visually. Here we define a measurement to be a Hit when conditions as in (17a) and (17b) are satisfied.

$$\left|W1_{User} - Wall1\right| < 2\,mm \quad (17a)$$

and, $$\left|W2_{User} - Wall2\right| < 2\,mm \quad (17b)$$

A typical ultrasound echo signal received from one human volunteer is shown in Fig. 8. The wall-detection Hit-rate during in-vivo measurements is illustrated in Fig. 9. It can be seen from Fig. 9, that if the algorithm analyses more than 10 frames in every measurement, it can reach a Hit-rate of more than 80%.

### B. Arterial compliance values measured in-vivo

Compliance and distensibility for the same volunteers were calculated by using equations (11), (12), (13) and (14) and the values are listed in Table I. A typical distension waveform is shown in fig. 10.

TABLE I. **Compliance and Distensibility Measurements for a Few Volunteers.**

| Vol (Age) | $\langle \Delta D \rangle$ (μm) | $\Delta P$ (mm Hg) | $\langle D_d \rangle$ (mm) | Compliance $(\frac{\mu m}{\text{mm Hg}})$ | Distensibility $(\frac{10^{-3}}{\text{mm Hg}})$ |
|---|---|---|---|---|---|
| A (23) | 448 | 40 | 5.41 | 11.20 | 2.1 |
| B (27) | 388 | 38 | 6.60 | 10.21 | 1.6 |
| C (30) | 400 | 34 | 5.76 | 11.76 | 2.0 |
| D (24) | 439 | 33 | 6.47 | 13.30 | 2.1 |

## VII. Conclusion

An imageless system for automated evaluation of arterial compliance has been presented. An algorithm for identification of approximate arterial wall locations to provide real-time assistance to the operator in placement of the probe has been demonstrated. The performance of the wall identification algorithm has been thoroughly characterized by simulation studies. The wall-detection algorithm could easily identify the arterial wall, with a Hit-rate in excess of 90 %, at SNR levels as low as 5 dB, in the normal expected wall-motion frequency range of 0.6 - 4 Hz. The wall detection algorithm achieved Hit-rates greater than 80 % even during in-vivo measurements performed by untrained personnel. Compliance was estimated for a few human volunteers under experimental settings which clearly demonstrated the utility of the device as an alternative tool for arterial compliance measurement. Elaborate testing of the system under a clinical environment is currently in progress. The use of automated algorithms to identify and track artery wall motion enables the device to be used by untrained personnel. Thus, the arterial compliance evaluation system presented here could pave the way for an effective and inexpensive cardiovascular screening tool.

## References

[1] S. Laurent *et al.*, "Expert consensus document on arterial stiffness : Methodological issues and clinical applications,"*European Heart Journal*, vol. 27, pp. 2588-2605, 2006.

[2] S. Mandal., *et al*, "Prevalence of Ischemic Heart Disease Among Urban Population of Siliguri, West Bengal," *Indian Journal of Community Medicine*, vol. 34, pp. 19-23, January 2009.

[3] R. Tavoos, M. Manijhe, V. Alireja and R. Abdorrazzagh, "Extraction of instantaneous changes in arterial walls with sequential ultrasound images," *Journal of Medical Ultrasonics*, vol.38, no. 2, pp. 81-87, April 2011.

[4] J. Joseph and V. Jayashankar, "A virtual instrument for automated measurement of arterial compliance," *ASME Journal of Medical Devices*, vol. 4, no. 4, art.045004, 2010.

[5] J. Krejza *et al.*,"Carotid artery diameter in men and women and the relation to body and neck size," *Stroke*, vol. 37, pp. 1103-1105, February, 2006.

[6] A. Abbate, N. Nguyen, S. LaBreck and T. Nelligan, "Ultrasonic signal processing algorithms for the characterisation of thin multilayers," *The e-Journal of Nondestructive testing*, vol. 7, no. 10, 2002.